THE JOURNAL OF BIOLOGICAL CHEMISTRY VOL. 290, NO. 3, pp. 1874–1884, January 16, 2015

Phosphorylation of Merkel Cell Polyomavirus Large Tumor Antigen at Serine 816 by ATM Kinase Induces Apoptosis in Host Cells*

Received for publication, July 8, 2014, and in revised form, November 5, 2014 Published, JBC Papers in Press, December 5, 2014, DOI 10.1074/jbc.M114.594895

Jing Li[‡], Jason Diaz[§], Xin Wang[¶], Sabrina H. Tsang[§], and Jianxin You[§1]

From the [‡]The Wistar Institute, Philadelphia, Pennsylvania 19104, the [§]Department of Microbiology, University of Pennsylvania Perelman School of Medicine, Philadelphia, Pennsylvania 19104, and the [¶]Department of Molecular Genetics, Lerner Research Institute, Cleveland, Ohio 44295

Background: Phosphorylation regulates Merkel cell polyomavirus (MCV) large tumor antigen (LT) activity.
Results: MCV LT is phosphorylated by ATM kinase at Ser-816.
Conclusion: Ser-816 phosphorylation by ATM allows MCV LT to arrest cell growth and induce apoptosis.
Significance: Ser-816 phosphorylation-induced apoptosis may explain why the C-terminal domain of LT is negatively selected in MCV-related tumors.

Merkel cell carcinoma is a highly aggressive form of skin cancer. Merkel cell polyomavirus (MCV) infection and DNA integration into the host genome correlate with 80% of all Merkel cell carcinoma cases. Integration of the MCV genome frequently results in mutations in the large tumor antigen (LT), leading to expression of a truncated LT that retains pRB binding but with a deletion of the C-terminal domain. Studies from our laboratory and others have shown that the MCV LT C-terminal helicase domain contains growth-inhibiting properties. Additionally, we have shown that host DNA damage response factors are recruited to viral replication centers. In this study, we identified a novel MCV LT phosphorylation site at Ser-816 in the C-terminal domain. We demonstrate that activation of the ATM pathway stimulated MCV LT phosphorylation at Ser-816, whereas inhibition of ATM kinase activity prevented LT phosphorylation at this site. *In vitro* phosphorylation experiments confirmed that ATM kinase is responsible for phosphorylating MCV LT at Ser-816. Finally, we show that ATM kinase-mediated MCV LT Ser-816 phosphorylation may contribute to the anti-tumorigenic properties of the MCV LT C-terminal domain.

Merkel cell polyomavirus (MCV)[2] is a recently identified polyomavirus that is associated with a highly aggressive skin cancer, Merkel cell carcinoma (MCC) (1, 2). MCV is associated with ~80% of MCC cases (1, 3, 4). MCC metastasizes rapidly. It is one of the most aggressive skin cancers, with an extremely high mortality rate of 33%, exceeding that of melanoma (5), and <45% 5-year survival rate (6). The incidence of MCC increased from 1.5 to 6/million people between 1986 and 2006, and ~1500 new cases of MCC are diagnosed each year in the United States (7, 8). Epidemiological surveys of anti-MCV antibodies and sequencing analyses of healthy human skin have indicated that MCV may represent a natural component of the human skin microflora (9–11).

Like other polyomaviruses, MCV encodes a single early gene, the tumor antigen. The MCV tumor antigen is multiply spliced into the large tumor antigen (LT), the small tumor antigen, 57kT, and ALTO (alternate frame of the large T open reading frame) (12, 13). Similar to other polyomaviruses, the multifunctional MCV LT protein is involved in a variety of processes, including viral genome replication and host cell cycle manipulation (14–16).

MCV LT contains conserved features of other polyomavirus LT proteins, such as conserved region 1, a DnaJ domain that interacts with Hsc70 family members, an L*X*C*X*E pRb-binding motif, an origin-binding domain, and a helicase/ATPase domain required for viral DNA replication (3, 12). The T antigens from several polyomaviruses have oncogenic activity. Notably, the SV40 large and small T antigens can transform a variety of rodent and human cells (17, 18). In addition, LT from SV40, as well as the human JC and BK polyomaviruses, can bind to pRb and p53 tumor suppressor proteins (19–22). MCV LT can bind specifically to pRb (3, 23). Although there are two potential p53-binding motifs in the MCV LT C-terminal domain, there appears to be no direct interaction between MCV LT and p53 (24, 25). Interestingly, the MCV genome is commonly clonally integrated into MCC tumor cell genomes. Almost all MCV LTs expressed from the integrated MCV genomes harbor nonsense mutations, which result in expression of a truncated LT that retains the N-terminal pRb-binding motif but has a deletion of the C-terminal DNA-binding and helicase domains (3). It has been postulated that these truncated LT proteins arise because replication of the integrated viral genome by full-length MCV LT may instigate a debilitating amount of DNA damage due to abortive replication at the integrated viral origin (3). The identification of a tumor with

* This work was supported, in whole or in part, by National Institutes of Health Grants R01CA148768, R01CA142723, and 3R01CA142723-05S1.
[1] To whom correspondence should be addressed: Dept. of Microbiology, University of Pennsylvania Perelman School of Medicine, 201C Johnson Pavilion, 3610 Hamilton Walk, Philadelphia, PA 19104-6076. Tel.: 215-573-6781; Fax: 215-573-9557; E-mail: jianyou@mail.med.upenn.edu.
[2] The abbreviations used are: MCV, Merkel cell polyomavirus; MCC, Merkel cell carcinoma; LT, large tumor antigen; DDR, DNA damage response; IIT, IgG-IgG-tobacco etch virus; CIP, calf intestinal alkaline phosphatase; TBST, TBS/Tween.

intact full-length LT but a mutated viral origin sequence supports this hypothesis (26). Later studies have since suggested that the C-terminal helicase domain may contain other functions that oppose tumorigenesis (16, 24). Our previous work indicated that expression of full-length MCV LT activates a dramatic DNA damage response (DDR) that is antagonistic to tumorigenesis; this activity activates p53 and induces a growth-inhibiting phenotype (16). Additionally, Cheng *et al.* (24) reported that expression of the C-terminal 100 residues of MCV LT inhibits the growth of several different cell types. These studies support a model in which the C-terminal domain must be deleted in tumor cells to both limit viral replication from the integrated viral genomes and eliminate growth-arresting properties intrinsic to the C-terminal domain of LT. How the MCV C-terminal 100 residues accomplish this growth-arresting function is not clearly understood.

In addition to being stimulated by MCV LT expression, work from our laboratory has shown that components of the host DDR are recruited to viral replication centers (27). These factors are necessary to support MCV genome replication (27), but their mechanism of action is not understood.

Protein phosphorylation of serines, threonines, and tyrosines is one of the most common methods for regulating protein function. Phosphorylation of SV40 LT on both serine and threonine residues plays an important role in regulating LT function. Phosphorylation of SV40 LT Ser-120 and Ser-123 inhibits viral replication, whereas phosphorylation of Thr-124 enhances replication by activating the DNA-binding domain and stimulating double-hexamer activity (28–32). Phosphorylation of Thr-701 is required for binding to the host FBW7 γ-isoform, which regulates SV40 LT protein stability (33). A recent report from our laboratory identified Thr-271, Thr-297, and Thr-299 as phosphorylation sites on MCV LT (34). In that report, we demonstrated that phosphorylation of Thr-297 and Thr-299 regulates MCV LT-mediated replication of the viral DNA. In the present study, we identified a novel MCV LT phosphorylation site at Ser-816. We demonstrate that this site was phosphorylated by ATM (ataxia telangiectasia mutated) kinase, a key component of the host DDR activated primarily by dsDNA breaks (35). Activation of ATM kinase by etoposide increased MCV LT phosphorylation at Ser-816. In contrast, ATR (ataxia telangiectasia and Rad3-related) kinase was unable to robustly phosphorylate MCV LT. Expression of wild-type MCV LT inhibited cell proliferation and also induced several cell lines to undergo apoptosis. Expression of the serine-to-alanine substitution mutant MCV LT S816A partially rescued this growth inhibition and also inhibited the induction of apoptosis. This study reveals that MCV LT is a substrate of ATM kinase and that phosphorylation at Ser-816 contributes to the regulation of host cell proliferation and apoptosis.

EXPERIMENTAL PROCEDURES

Cell Culture, Cell Lines, and Transfection—U2OS cells were maintained in McCoy's 5A medium (Invitrogen) containing 10% fetal bovine serum (HyClone). C33A, HeLa, 293, and 293T cells were maintained in DMEM (Invitrogen) containing 10% fetal bovine serum. FuGENE 6 transfection reagent (Roche Applied Science) and Lipofectamine 2000 (Invitrogen) reagents were used to transfect U2OS, C33A, and HeLa cells following the manufacturers' instructions. The calcium phosphate method was used for 293 and 293T transfections as described previously (14).

Recombinant Plasmid Construction—Plasmids pcDNA-MCV LT(1–211), pcDNA4C-MCV LT(212–440), pcDNA4C-MCV LT(1-440), pcDNA4C-MCV LT(212–817), pcDNA4C-MCV LT(1-817), pEGFPC1-MCV LT(1–440), pEGFPC1-MCV LT(441–817), pEGFPC1-MCV LT(1–817), pcDNA4C-IIT-MCV LT(1–817), pLPCX-Cherry-LacI, pLPCX-MCV LT(1–817), and pGEX-MCV LT have been described previously (14, 16). To generate pcDNA4C-MCV LT S816A, pEGFPC1-MCV LT S816A, or pLPCX-MCV LT S816A, site-directed mutagenesis was performed with QuikChange PCR (Stratagene) following the manufacturer's instructions using pcDNA4C-MCV LT(1–817), pEGFPC1-MCV LT(1–817), or pLPCX-MCV LT(1–817) as a template. For pcDNA4C-IIT-MCV LT S816A, the IIT tag (containing two IgG-binding domains and a tobacco etch virus cleavage site) was subcloned into pcDNA4C-MCV LT(1–817) using the KpnI fragment from the pcDNA4c-IIT-MCV LT(1–817) construct described previously (14). All constructs were confirmed by restriction enzyme digestion and DNA sequencing. The pTIH plasmid encoding SV40 LT was a kind gift from Chris Buck (National Institutes of Health).

Antibodies and Chemicals—The following antibodies were used for immunoblotting: mouse anti-MCV LT (Santa Cruz Biotechnology); mouse anti-Xpress (Invitrogen); rabbit anti-phosphorylated ATM Ser-1981, rabbit anti-ATR (Abcam), and mouse anti-proliferating cell nuclear antigen (Abcam); rabbit anti-ATM, rabbit anti-phosphorylated Chk1 Ser-345, HRP-conjugated goat anti-mouse, and HRP-conjugated goat anti-rabbit (Cell Signaling); mouse anti-actin (Chemicon); and mouse anti-GAPDH (United States Biological). Mouse anti-ATM (Sigma-Aldrich), rabbit anti-ATR (Abcam), and normal rabbit IgG and normal mouse IgG (Millipore) antibodies were used for immunoprecipitations.

Etoposide, wortmannin, NU6027, caffeine, and puromycin were purchased from Sigma-Aldrich. NU7441 was purchased from Tocris Bioscience. KU55933 was purchased from EMD Millipore. AZD7762 was purchased from Selleck Chemicals. Calf intestinal alkaline phosphatase (CIP) was purchased from New England Biolabs. Phycoerythrin-conjugated annexin V was purchased from BioVision. AcTEV protease was obtained from Invitrogen. Western Lightning Plus ECL solution was purchased from PerkinElmer Life Sciences.

CIP Assay—At 48 h post-transfection, cells were lysed in lysis buffer (50 mM Tris-HCl (pH 8.0), 150 mM NaCl, 10% glycerol, 1% Nonidet P-40, 5 mM $MgCl_2$, 1 mM DTT, and protease inhibitors) and passed five times through a 26-gauge needle. Lysates were incubated on ice for 20 min with occasional vortexing and then spun down at 5000 rpm for 5 min at 4 °C. Cleared supernatants were collected. A Bradford assay was performed to determine protein concentration, and lysates were diluted to 1 mg/ml with lysis buffer. A 100-μg aliquot of lysate was used for CIP treatment: NEBuffer 3 was added to the lysate to a final concentration of 1× buffer, and the solution was incubated at 37 °C for 5 min. The samples were then treated with 50 units of

CIP for 30 min at 37 °C. Samples were boiled in sample buffer and immunoblotted.

Annexin V Staining—C33A cells were transfected with pEGFPC1 (vector), pEGFPC1-MCV LT, or pEGFPC1-MCV LT S816A. 24 h later, cells were washed with binding buffer (10 mM HEPES (pH 7.4), 140 mM NaCl, and 2.5 mM $CaCl_2$), stained with phycoerythrin-conjugated annexin V for 10 min, washed once more with binding buffer, and fixed with 3% paraformaldehyde for 20 min. Nuclei were counterstained with DAPI.

Microscopy and Image Analysis—All immunofluorescent images were collected using an Olympus IX81 inverted fluorescence microscope connected to a QImaging Fast 1394 high-resolution charge-coupled device camera. Images were analyzed and presented using SlideBook 5.0 software (Intelligent Imaging Innovations, Inc.). The scale bars were added using ImageJ software.

Western Blotting—At 36 h post-transfection, cells were lysed 10 mM HEPES (pH 7.9), 300 mM NaCl, 3 mM $MgCl_2$, 1 mM DTT, 1 mM PMSF, 3 mM sodium butyrate, 1 mM NaF, and 100 μM Na_3VO_4 supplemented with protease inhibitor mixtures (Roche Applied Science) and Ser/Thr protein phosphatase inhibitor mixtures (Sigma) and passed 10 times through a 26-gauge needle. After a 20-min incubation on ice with occasional vortexing, the soluble and insoluble fractions were separated by centrifugation at 5000 rpm for 5 min at 4 °C. The supernatant (20 μg) was resolved by SDS-PAGE. 1 mM NaF and 100 μM Na_3VO_4 were added to electrophoresis buffer and transfer buffer to inhibit phosphatase activity. Membranes were blocked in 5% TBST/milk for 1 h at room temperature and incubated in TBST/milk containing primary antibodies at 4 °C overnight. For anti-phosphoprotein antibodies, TBST/BSA was used instead of TBST/milk. Membranes were then incubated with HRP-conjugated secondary antibodies in TBST/milk for 1 h at room temperature. Western blots were developed using ECL solution, and images were captured using a Fuji imaging system.

Retrovirus Production and Stable Cell Line Construction—293T cells were cultured in 10-cm dishes to reach 95–100% confluency. pLPCX-based plasmids (pLPCX-Cherry-LacI, pLPCX-MCV LT(1–817), and pLPCX-MCV LT(1–817) S816A), pCMV-VSV-G, and pMD-gagpol were cotransfected into 293T cells using Lipofectamine 2000 transfection reagent. After 48 h, the packaged retroviruses in the supernatant were harvested and filtered through a 0.45-μm filter before transducing C33A and HeLa cells. At 48 h post-infection, the transduced cells were selected using 0.625 or 1 μg/ml puromycin, respectively, for 4 days. Expression of MCV LT was confirmed by immunofluorescence staining and Western blotting, and the selected cells were maintained as stable cell lines in DMEM supplemented with puromycin.

In Vitro Phosphorylation Assay—To activate ATM and ATR, U2OS cells were treated for 4 h with 4 μM etoposide, which induces dsDNA breaks. Treated cells were harvested; resuspended in 10 mM HEPES (pH 7.9), 10 mM KCl, 0.1 mM EDTA, 0.1 mM EGTA, 1 mM DTT, 0.2 mM PMSF, 3 mM sodium butyrate, 1 mM NaF, and 100 μM Na_3VO_4 supplemented with protease inhibitor mixtures and Ser/Thr protein phosphatase inhibitor mixtures; and incubated on ice for 10 min. Nonidet P-40 was added to final concentration of 0.02%, and cells were vortexed for 10 s. Nuclei were separated by centrifugation at 4000 rpm for 10 min at 4 °C. Isolated nuclei were lysed in 20 mM HEPES (pH 7.9), 0.5 M NaCl, 1 mM EDTA, 1 mM EGTA, 1 mM DTT, 0.2 mM PMSF, 3 mM sodium butyrate, 1 mM NaF, and 100 μM Na_3VO_4 supplemented with protease inhibitor mixtures and Ser/Thr protein phosphatase inhibitor mixtures and passed 10 times through a 22-gauge needle, followed by rotation at 4 °C for 1 h. Nuclear extracts were isolated by centrifugation at 14,000 rpm for 10 min at 4 °C.

Nuclear extracts (500 μg) were mixed with 10 μg of rabbit anti-ATM, 10 μg of mouse anti-ATR, or 10 μg of normal rabbit IgG antibody together with 10 μg of normal mouse IgG antibody. Nuclear extracts and the antibody mixture was rotated at 4 °C for 2 h, followed by addition of 10 μl of protein G-agarose beads (Invitrogen). Mixtures were rotated for an addition 1 h at 4 °C. Purified proteins on resin were washed four times with KCl buffer (20 mM Tris (pH 8.0), 10% glycerol, 5 mM $MgCl_2$, 0.1% Tween 20, 150 mM KCl, 0.1 mM PMSF, 3 mM sodium butyrate, 1 mM NaF, and 100 μM Na_3VO_4 supplemented with protease inhibitor mixtures and Ser/Thr protein phosphatase inhibitor mixtures). The resin was then equilibrated once with kinase buffer (20 mM HEPES (pH 7.6), 50 mM NaCl, 10 mM $MgCl_2$, 1 mM DTT, 20 mM $MnCl_2$, and 1 mM NaF). IIT-MCV LT was purified as described previously (16) and treated with CIP as described above. MCV LT was cleaved with AcTEV protease following the manufacturer's instructions.

10 μl of equilibrated resin with purified proteins was mixed with 30 μl of kinase buffer, 1 μg of purified MCV LT, 200 μM ATP, and 0.5 μl of 3000 Ci/mmol [γ-^{32}P]ATP. Kinase assay was performed at room temperature or 37 °C for 30 min. Proteins were separated by SDS-PAGE, and the gel was subsequently dried at 80 °C for 30 min. Autoradiography was performed as described previously (14).

GST Pulldown Assay—BL21(DE3)pLysS *Escherichia coli* cells were transformed with pGEX-MCV LT or pGEX vector. Bacteria were lysed in 10 mM Tris-HCl (pH 8.0), 50 mM NaCl, 0.4 mg/ml lysozyme, 2 mM DTT, and 0.1 mM EDTA supplemented with protease inhibitors) before running through Q-Sepharose and SP-Sepharose columns (Sigma). The SP-Sepharose column was washed with 50 mM Tris-HCl (pH 8.0), 150 mM NaCl, 2 mM DTT, and 0.1 mM EDTA supplemented with protease inhibitors before elution with the same buffer adjusted to 400 mM NaCl. The elution mixture was then incubated with GSH-agarose (Sigma) at 4 °C for 2 h. GSH-agarose was washed five times with 20 mM Tris-HCl (pH 8.0), 5 mM $MgCl_2$, 0.1% Tween 20, and 100 mM KCl supplemented with protease inhibitors. Bound proteins were used for GST pulldown assay. Briefly, U2OS nuclear extracts was prepared as described previously (36) and incubated with beads bound to GST or GST-LT at 4 °C overnight. The beads were washed three times with 0.5 ml of 0.1 M KCl buffer and eluted with 30 μl of SDS-PAGE sample buffer.

Clonogenic Assay—C33A cells stably expressing Cherry-LacI, LT(1–817), or LT(1–817) S816A were plated in triplicate at 5×10^3 cells/well in a 6-well plate and cultured in DMEM with 0.625 μg/ml puromycin for 10 days. The cells were then fixed with methanol and stained with 0.5% methylene blue.

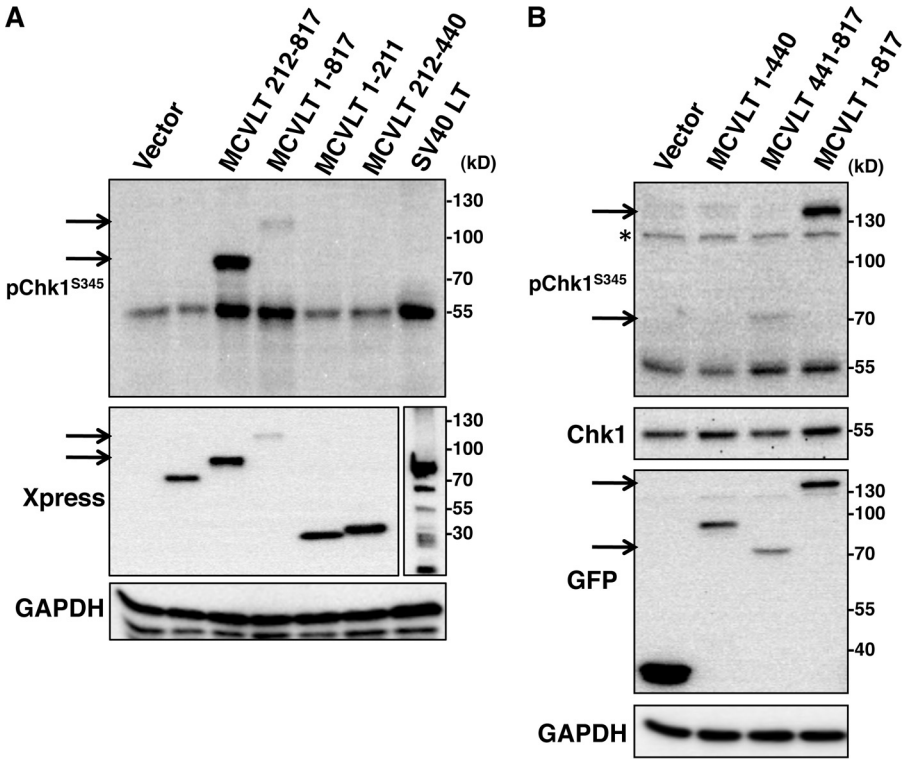

FIGURE 1. **Anti-phospho-Chk1 Ser-345 antibody cross-reacts with MCV LT.** *A*, U2OS cells were transfected with pcDNA4C (*Vector*), pcDNA4C encoding Xpress-tagged MCV LT molecules as indicated, or pTIH encoding SV40 LT. At 36 h post-transfection, cells were lysed and immunoblotted with the indicated antibodies. *Arrows* indicate cross-reactive bands corresponding to the molecular masses of the transfected LT molecules. *B*, U2OS cells were transfected with pEGFPC1 (*Vector*) or pEGFPC1 encoding MCV LT molecules as indicated. At 36 h post-transfection, cells were lysed and immunoblotted with the indicated antibodies. *Arrows* indicate cross-reactive bands matching the molecular masses of the transfected LT molecules as indicated in *A*. The *asterisk* indicates an additional cross-reactive band present in U2OS cells regardless of LT expression.

RESULTS

MCV LT Is Phosphorylated at Ser-816—In our previous study, we found that either MCV infection or transfection of MCV genomes into cells activated both ATM and ATR kinases, whereas ectopic expression of only MCV LT primarily induced the ATR-Chk1 DDR pathway in U2OS cells (16). Interestingly, in these immunoblot experiments, we also discovered that the anti-phospho-Chk1 Ser-345 antibody not only detected phospho-Chk1 Ser-345 but also recognized protein bands with molecular masses that match those of transfected LT(1–817), LT(212–817), GFP-LT(441–817), and GFP-LT(1–817), respectively (Fig. 1, *A* and *B*, *arrows*). This cross-reactivity was observed for all MCV LT truncation mutants retaining the C-terminal ~400 amino acids (Fig. 1, *A* and *B*). These cross-reactive bands were also detected in C33A and HeLa cells (data not shown). This antibody also recognized another cross-reactive band of ~120 kDa in all samples, regardless of LT expression (Fig. 1*B*, *asterisk*). SV40 LT also activated phospho-Chk1 Ser-345 in U2OS cells (16), but there were no cross-reactive bands detected in the SV40 LT sample (Fig. 1*A*). Because the cross-reactive bands (marked with an *asterisk*) had similar molecular masses as the ectopically expressed LTs in those samples, we suspected that the anti-phospho-Chk1 Ser-345 antibody was specifically cross-reacting with MCV LT.

To confirm that this cross-reaction was mediated by a true phosphorylation modification, lysates from U2OS cells transfected with pcDNA4C-MCV LT were treated with or without CIP for 30 min and analyzed by Western blotting. As shown in Fig. 2*A*, expression of LT(1–817) activated a robust phospho-Chk1 Ser-345 signal in U2OS cells, and there was again a cross-reactive band with a molecular mass of ~110 kDa, which matches the size of full-length MCV LT. Treatment with CIP significantly diminished both the phospho-Chk1 and 110-kDa cross-reactive signals (marked with an *arrow*) in the cell lysate (Fig. 2*A*). Interestingly, the other cross-reactive band of ~120 kDa (marked with an *asterisk*) was also diminished. This result suggests that the anti-phospho-Chk1 Ser-345 antibody recognizes a true phosphorylation modification on both the 110- and 120-kDa cross-reactive bands.

Chk1 is phosphorylated by ATR kinase at Ser-345 in a canonical (Ser/Thr)-Gln epitope that is commonly targeted by ATM and ATR kinases. Assuming that the cross-reactive band that was similar to transfected LT was indeed MCV LT, the data from Fig. 1 suggested that the phosphorylation site was within the C-terminal 400 amino acids. We compared the epitope recognized by the anti-phospho-Chk1 Ser-345 antibody with the C-terminal sequence of MCV LT and generated alanine substitutions of several potential phosphorylation sites. These point mutants were transfected into U2OS cells and immunoblotted with the anti-phospho-Chk1 Ser-345 antibody. Of all the sites analyzed, we found that mutagenesis of Ser-816 alone abolished MCV LT cross-reactivity with the anti-phospho-Chk1 Ser-345 antibody (Fig. 2*B* and data not shown). The 120-kDa cross-reactive band was unaffected when cells were transfected with this mutant LT. Taken together, these data demonstrate that MCV LT is phosphorylated at Ser-816 and that this phosphor-

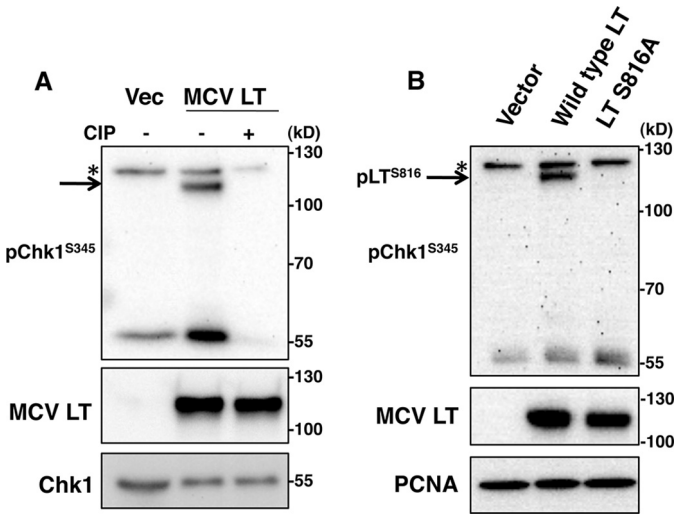

FIGURE 2. **MCV LT is phosphorylated at Ser-816.** *A*, U2OS cells were transfected with the pcDNA4C vector (*Vec*) or pcDNA4C-MCV LT. At 48 h post-transfection, cells were treated with (+) or without (−) CIP and analyzed by Western blotting. The *asterisk* and *arrow* indicate cross-reactive bands as described in the legend to Fig. 1. *B*, U2OS cells were transfected with pcDNA4C (*Vector*), pcDNA4C-MCV LT(1–817) (*Wild type LT*), or pcDNA4C-MCV LT(1–817) S816A (*LT S816A*). At 48 h post-transfection, cells were harvested, and proteins were analyzed by Western blotting with the indicated antibodies. The *asterisk* and *arrow* indicate cross-reactive bands as described in the legend to Fig. 1. *PCNA*, proliferating cell nuclear antigen.

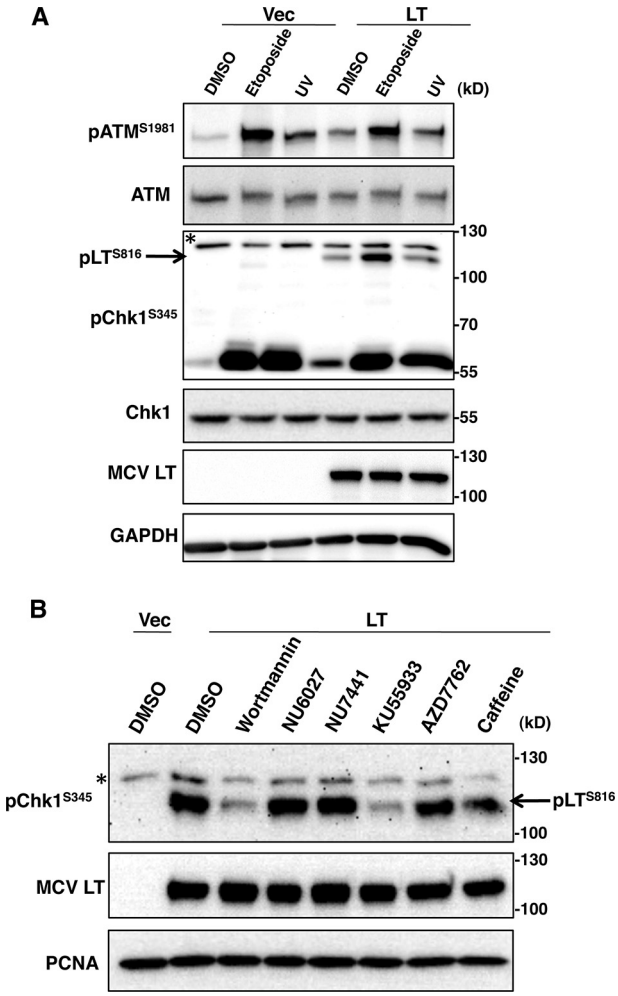

FIGURE 3. **ATM kinase phosphorylates MCV LT at Ser-816.** *A*, U2OS cells were transfected with the pcDNA4C vector (*Vec*) or pcDNA4C-MCV LT (*LT*). At 44 h post-transfection, cells were treated with 4 μM etoposide for 4 h or 10 J of UVC light. Cells were then harvested and analyzed by Western blotting with the indicated antibodies. The *asterisk* and *arrow* indicate cross-reactive bands as described in the legend to Fig. 1. *B*, U2OS cells were transfected with pcDNA4C (*Vec*) or pcDNA4C-MCV LT(1–817) (*LT*). At 44 h post-transfection, cells were treated with dimethyl sulfoxide (*DMSO*), 20 μM wortmannin, 20 μM NU6027, 1 μM NU7441, 10 μM KU55933, 10 nM AZD7762, or 10 mM caffeine for 6 h. Cells were then harvested, and proteins were analyzed by Western blotting with the indicated antibodies. The *asterisk* and *arrow* indicate cross-reactive bands as described in the legend to Fig. 1. *PCNA*, proliferating cell nuclear antigen.

ylation is specifically recognized by the anti-phospho-Chk1 Ser-345 antibody. The 120-kDa band (marked with an *asterisk*) is likely a cellular phosphoprotein that is also recognized by this antibody; however, we chose to focus the remainder of our study on MCV LT.

Activation of ATM Stimulates MCV LT Ser-816 Phosphorylation—Having identified Ser-816 as a phosphorylation site of MCV LT, we next sought to determine which kinase or kinase pathway is responsible for this modification. Our previous data showed that MCV infection and MCV genome transfection activate both ATM and ATR DDR pathways. In contrast, ectopic expression of MCV LT alone predominantly activates ATR and only weakly activates ATM (16, 27). Additionally, we have reported that components of the host DDR pathways are recruited to viral replication centers and that their activity is required for efficient replication (27). We wondered whether components of these DDR pathways could be responsible for LT Ser-816 phosphorylation.

We first used etoposide or UV light to activate either the ATM or ATR pathway, respectively, and tested whether phosphorylation of LT was altered. U2OS cells were transfected with pcDNA4C (vector) or pcDNA4C-MCV LT. At 48 h post-transfection, cells were treated with either 4 μM etoposide for another 4 h or treated with 10 J of UVC light. The cells were then harvested for Western blot analysis. As shown in Fig. 3*A*, expression of LT induced a mild activation of both ATM Ser-1981 phosphorylation and Chk1 Ser-345 phosphorylation, a surrogate of ATR activation (compare the *fourth lane* with the *first lane*). Etoposide treatment, which activates primarily ATM kinase, induced a dramatic activation of ATM Ser-1981 phosphorylation, as well as LT Ser-816 phosphorylation (Fig. 3*A*, *fifth lane*). In contrast, UV light treatment, which activates predominantly ATR, caused a much smaller degree of ATM phosphorylation and very little activation of LT Ser-816 phosphorylation compared with dimethyl sulfoxide treatment (Fig. 3*A*, compare the *sixth lane* with the *fourth lane*). These results demonstrated that activation of the host ATM DDR pathway could stimulate phosphorylation of MCV LT at Ser-816. Robust phosphorylation of Chk1 Ser-345 was seen with both etoposide and UV treatments, indicating either that ATR was activated in both settings or that the robust activation of ATM during etoposide treatment allowed it to phosphorylate Chk1 through cross-talk (37–40).

Inhibition of ATM Prevents MCV LT Ser-816 Phosphorylation—We next sought to determine which component(s) of the host DDR was responsible for phosphorylating MCV LT. We tested a panel of chemical inhibitors to screen for the possible kinases that phosphorylate MCV LT at Ser-816. U2OS cells

were transfected with pcDNA4C (vector) or pcDNA4C-MCV LT. 44 h later, cells were treated with dimethyl sulfoxide, wortmannin, NU6027, NU7441, KU55933, AZD7762, or caffeine for another 6 h. The cells were harvested for Western blot analysis. As shown in Fig. 3*B*, the expression level of LT was constant with the different drug treatments. MCV LT-transfected cell lysates showed phosphorylated MCV LT Ser-816 bands at ~110 kDa; however, the band density changed with the various drug treatments (Fig. 3*B*). Caffeine, which inhibits both ATM and ATR, reduced LT Ser-816 phosphorylation to a small extent (Fig. 3*B*). Wortmannin, which acts as a broad PI3K inhibitor that inhibits DNA-dependent protein kinase, ATM, and ATR, efficiently inhibited MCV LT Ser-816 phosphorylation (Fig. 3*B*). On the other hand, the ATR inhibitor NU6027, the DNA-dependent protein kinase inhibitor NU7441, and the Chk1 inhibitor AZD7762 did not affect LT phosphorylation (Fig. 3*B*). These results suggest that the ATM pathway is likely important for LT Ser-816 phosphorylation. Further supporting this notion, the ATM inhibitor KU55933 dramatically reduced LT Ser-816 phosphorylation (Fig. 3*B*). These experiments were repeated in C33A cells with similar results (data not shown). Taken together, these data suggest that ATM is likely the kinase that phosphorylates MCV LT at Ser-816.

ATM Kinase Binds and Phosphorylates MCV LT at Ser-816 in Vitro—We then performed *in vitro* phosphorylation experiments to more directly confirm that ATM kinase phosphorylates MCV LT at Ser-816. IIT affinity-tagged wild-type MCV LT or MCV LT S816A was purified from 293 cells and treated with CIP to remove phosphorylation modifications. In parallel, U2OS cells were stimulated with etoposide to activate the host DDR, and either the ATM or ATR kinase was immunoprecipitated from nuclear extracts (Fig. 4*A*). ATM or ATR was then immunoprecipitated, immobilized on Sepharose beads, and incubated with radiolabeled ATP and equal amounts of either wild-type LT or LT S816A protein in kinase reaction buffer. Only wild-type LT incubated with immunopurified ATM demonstrated significant phosphorylation; incubation with ATR did not show detectable activity above background levels (Fig. 4*A*). This was true when the *in vitro* phosphorylation reaction was performed at either room temperature or 37 °C. LT S816A was not phosphorylated by either the ATM or ATR kinase, regardless of temperature (Fig. 4*A*). We also confirmed that LT could interact with ATM by pulling down ATM kinase from U2OS nuclear extracts using immobilized, bacterially derived LT (Fig. 4*B*). This binding was clearly evident even with a relatively small amount of LT (Fig. 4*B*, compare the *GST* and *GST-LT lanes* in the Coomassie Brilliant Blue stain). Together with the kinase inhibitor screen shown in Fig. 3*B*, these data strongly suggest that ATM is the major kinase that phosphorylates MCV LT at Ser-816.

Prevention of MCV LT Ser-816 Phosphorylation Partially Rescues the MCV LT Growth-inhibiting Effect—We next sought to better understand the physiological function of the ATM-mediated MCV LT Ser-816 phosphorylation. We were unable to find defects in genome replication or viral gene transcription for MCV LT S816A (data not shown). Our previous study demonstrated that the C-terminal portion of LT activates p53 and promotes growth inhibition (16). Cheng *et al.* (24) also reported that the C-terminal 100 amino acids of MCV LT have a cell growth-inhibiting effect. The underlying mechanism of these findings was not completely established. Because the C-terminal domain of MCV LT is sufficient for DDR activation (16) and because Ser-816 lies within the C-terminal 100-amino acid region of MCV LT, we asked whether Ser-816 phosphorylation plays a role in the cell growth-inhibiting function of the MCV LT C terminus. We generated C33A cells stably expressing wild-type MCV LT, MCV LT S816A, or Cherry-LacI as a negative control. Using these cell lines, we performed a clonogenic assay to detect the long-term effect of MCV LT and MCV LT S816A on cell proliferation. The same number of stable C33A cells were seeded in 6-well dishes and cultured for 10 days under puromycin selection. As shown in Fig. 5, the Cherry-LacI stable cell line formed a large number of colonies. As reported previously (16), expression of wild-type MCV LT caused a significant inhibition of cell growth, resulting in drastically reduced colony number after selection (Fig. 5). MCV LT S816A partially reversed this LT growth-inhibiting phenotype, allowing more colonies to be formed after the extended culture period (Fig. 5). This result suggests that blocking MCV LT Ser-816 phosphorylation can partially rescue LT growth-inhibiting activity, demonstrating the impact of MCV LT Ser-816 phosphorylation on cell proliferation.

MCV LT S816A Induces Less Apoptosis Compared with Wild-type MCV LT—We consistently observed that transfection of the MCV LT S816A construct led to less cell death compared with the wild-type MCV LT construct. The results of the clonogenic assay also suggested that MCV LT S816A might induce less cell death than wild-type MCV LT. We therefore tested both proteins for their ability to induce apoptosis. We performed annexin V staining to detect cells that express phosphatidylserine on the cell surface, which is an early marker of apoptosis (41). GFP-tagged MCV LT or MCV LT S816A was transfected into C33A cells. The transfected cells were stained with phycoerythrin-conjugated annexin V at 24 h post-transfection. Cells were then fixed, and nuclei were counterstained with DAPI. At this time point, ~0.2% of vector-transfected cells had annexin V staining, whereas 6.5% of MCV LT-transfected cells showed positive annexin V staining. However, only 3.8% of MCV LT S816A-transfected cells were annexin V-positive (Fig. 6, *A* and *B*). This result shows that MCV LT S816A has a decreased ability to induce cell death compared with MCV LT. Flow cytometry analysis also detected slightly more apoptotic cells with sub-G_1 fractions in wild-type MCV LT-transfected cells than in the MCV LT S816A samples (data not shown). These results are consistent with the observation that MCV LT can more potently inhibit cell proliferation compared with MCV LT S816A (Fig. 5).

To examine the differential activation of cell death by wild-type MCV LT and MCV LT S816A at the molecular level, we performed Western blot analyses to detect the apoptotic markers caspase-3 and PARP1. Caspase-3 is activated in both the extrinsic (death ligand) and intrinsic (mitochondrial) apoptotic pathways (42, 43). In the intrinsic activation pathway, cytochrome *c* from the mitochondria works in combination with caspase-9, Apaf1, and ATP to process procaspase-3 (44–46).

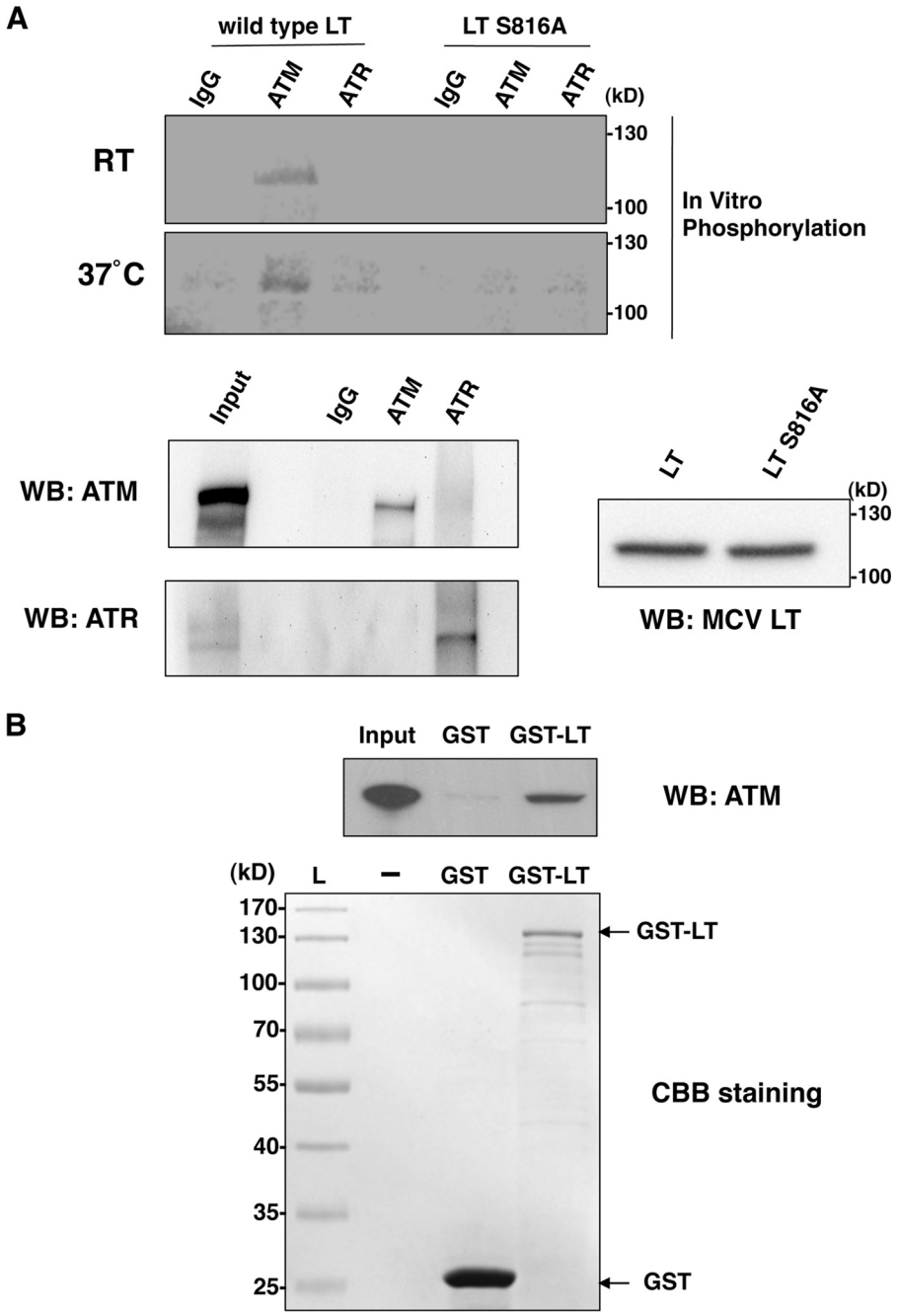

FIGURE 4. **ATM can bind and phosphorylate LT *in vitro*.** *A*, *in vitro* phosphorylation of MCV LT Ser-816 by ATM. Affinity-tagged MCV LT or MCV LT S816A was purified from 293 cells and treated with CIP. ATM and ATR proteins were immunoprecipitated from U2OS cells that had been treated with 4 μM etoposide for 4 h. Purified LT was then incubated with purified ATM or ATR in kinase reaction buffer supplemented with [γ-^{32}P]ATP. Reactions were performed at either room temperature (*RT*) or 37 °C for 30 min. Reactions were separated by SDS-PAGE and then either dried and exposed for autoradiography (*upper*) or Western-blotted (*WB*) for MCV LT (*lower right*). Immunopurified ATM and ATR proteins were Western-blotted with the indicated antibodies (*lower left*). *B*, GST-LT pulldown of ATM. U2OS nuclear extracts were mixed with either immobilized, bacterially derived GST or GST-LT protein. Input nuclear extract and pulldown samples were immunoblotted with anti-ATM antibody (*upper*). GST or GST-LT eluted from the glutathione resin was separated by SDS-PAGE and stained with Coomassie Brilliant Blue (*CBB*) (*lower*). *L*, molecular weight ladder; −, empty lane.

Proteolytic processing of the inactive zymogen into p17 and p12 fragments activates caspase-3. PARP1 is involved in the repair of DNA damage by adding poly(ADP-ribose) polymers to a variety of substrates in response to various cellular stresses (47). PARP1 is also a substrate for caspases; during the execution phase of apoptosis, PARP1 is specifically proteolyzed by caspase-3 to produce a 24-kDa N-terminal DNA-binding domain and an 89-kDa C-terminal catalytic fragment (48). Cleavage of PARP1 by caspases is considered to be a hallmark of apoptosis (49, 50).

We transfected either C33A or HeLa cells with pcDNA4C (vector), pcDNA4C-MCV LT, or pcDNA4C-MCV LT S816A. Cells were harvested at 30 h post-transfection and analyzed by Western blotting. As shown in Fig. 6 (*C* and *D*), the expression levels of MCV LT and MCV LT S816A were similar. Vector-transfected cells did not exhibit cleaved caspase-3 and showed

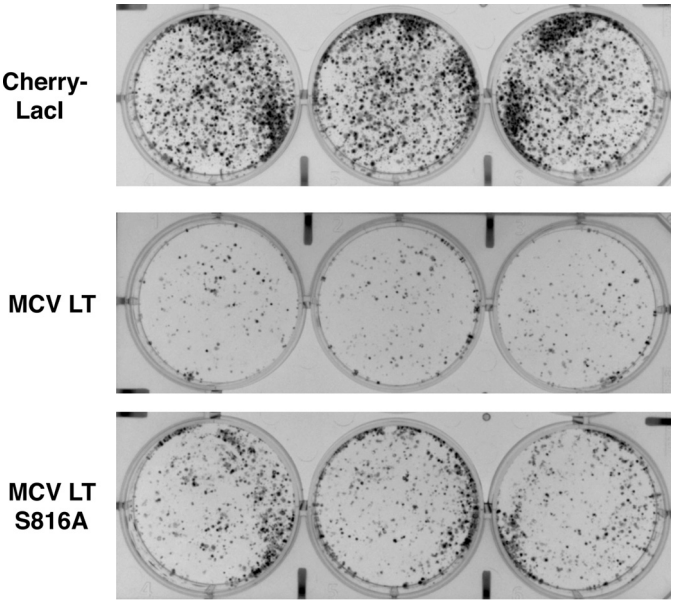

FIGURE 5. **C33A cells stably expressing MCV LT S816A form more colonies than cells stably expressing wild-type LT.** C33A cells stably expressing Cherry-LacI, MCV LT, or MCV LT S816A were seeded at 5000 cells/well in a 6-well plate. Cells were cultured for 10 days with 0.625 μg/ml puromycin. Colonies were fixed with methanol and stained with methylene blue. Data shown are representative of at least three experiments.

only the background level of cleaved PARP1, indicating little apoptosis under these conditions. Wild-type LT-transfected cells had less intact PARP1 but more cleaved PARP1 as well as more cleaved caspase-3 compared with the empty vector samples, confirming the induction of apoptosis. In contrast, the levels of cleaved PARP1 and cleaved caspase-3 in the MCV LT S816A-transfected cells were reduced to nearly the vector control level. These results are consistent with the observation that MCV LT-positive cells are more likely to undergo apoptosis than MCV LT S816A-positive cells (Fig. 6, *A* and *B*). These results support the rescue of the cell growth-inhibiting phenotype seen in the clonogenic assay (Fig. 5).

We also tested whether the S816E mutant would act as a phosphomimetic and presumably induce more apoptosis. Unfortunately, MCV LT S816E behaved identically to the alanine mutant and therefore was not a viable phosphomimetic (data not shown). This phenomenon has occasionally been reported for other phosphoproteins, including SV40 LT and MCV LT, at other phosphosites (34, 51). Taken together, these data suggest that phosphorylation of LT at Ser-816 contributes to growth arrest and apoptotic induction mediated by the C-terminal domain.

DISCUSSION

Most MCV-related MCC tumors examined thus far contain clonally integrated MCV genomes, which express truncated LT proteins without the C-terminal domain (3). This observation suggests a strong selective pressure to eliminate the C-terminal region of MCV LT during MCC tumor development. These tumor-specific mutations do not affect the LT pRb-binding domain or DnaJ domain (1). In fact, these LT mutants even have an increased affinity for pRb (25). Work from our laboratory and others suggests that the C-terminal domain of MCV LT might be negatively selected during tumorigenesis to eliminate growth-inhibiting properties encoded in this region (16, 24).

Our previous report showed that inhibition of cell proliferation by the C-terminal half of MCV LT is linked to its ability to activate the host DDR pathways (16). In those experiments, we consistently detected cross-reactivity of the anti-phospho-Chk1 Ser-345 monoclonal antibody when MCV LT constructs were expressed. In the present study, we explored the nature of this cross-reactivity. The cross-reactive bands correlated with the sizes of ectopically expressed, full-length MCV LT or LT C-terminal mutants (Fig. 1) and were sensitive to phosphatase treatment (Fig. 2*A*), making us suspect that this antibody recognized a phosphorylation modification on MCV LT. This cross-reaction seemed to be localized to the C-terminal half of the protein (Fig. 1). Alanine substitutions of candidate serines and threonines further identified Ser-816 as the target of phospho-Chk1 Ser-345 cross-reaction (Fig. 2*B*).

Our previous studies showed that MCV LT activates the host DDR proteins, which are recruited to actively replicating viral genomes (16, 27). The cross-reactive anti-phospho-Chk1 Ser-345 antibody was generated against Chk1 phosphorylated at Ser-345, an ATR kinase phosphorylation site. We therefore asked whether the DDR kinases were responsible for the phosphorylation of MCV LT at Ser-816. Activation of ATM kinase with etoposide caused a dramatic stimulation of MCV LT phosphorylation. On the other hand, UV treatment, which activates predominantly the ATR pathway, had little stimulating effect on MCV LT Ser-816 phosphorylation (Fig. 3*A*). A screen with multiple DDR kinase inhibitors further supported the hypothesis that ATM kinase is the predominant member of the DDR pathways responsible for this modification (Fig. 3*B*). *In vitro* phosphorylation of MCV LT with immunopurified ATM and ATR confirmed that ATM phosphorylates MCV LT at Ser-816, but ATR cannot (Fig. 4*A*). Additional pulldown experiments suggested that ATM and LT can indeed interact (Fig. 4*B*). Together with our published results (16, 27), the present study suggests that MCV not only is able to induce DDR in cells but can also take advantage of this DDR activity and recruit a cellular DDR kinase, ATM, to phosphorylate its own LT at Ser-816.

We next sought to understand the physiological role of this phosphorylation mark. Although Ser-816 lies C-terminal to the helicase domain, no effects were seen on viral genome replication or transcription (data not shown). We therefore asked whether LT Ser-816 phosphorylation contributes to the growth-inhibiting activity that is localized to the final 100 residues of this protein (24). Interestingly, the growth-inhibiting effect seen with wild-type LT was partially reversed with LT S816A in a clonogenic assay (Fig. 5). The cell proliferation phenotype was supported by an analysis of apoptosis during LT expression. Annexin V staining and Western blot analyses of caspase-3 and PARP1 cleavage showed that LT S816A induced less apoptosis in transfected cells (Fig. 6). These results demonstrated that the ATM-mediated phosphorylation of MCV LT at Ser-816 contributes to a mechanism that inhibits cell proliferation by inducing cell death.

Although this study established a direct functional interaction between ATM kinase and MCV LT, the precise role of this

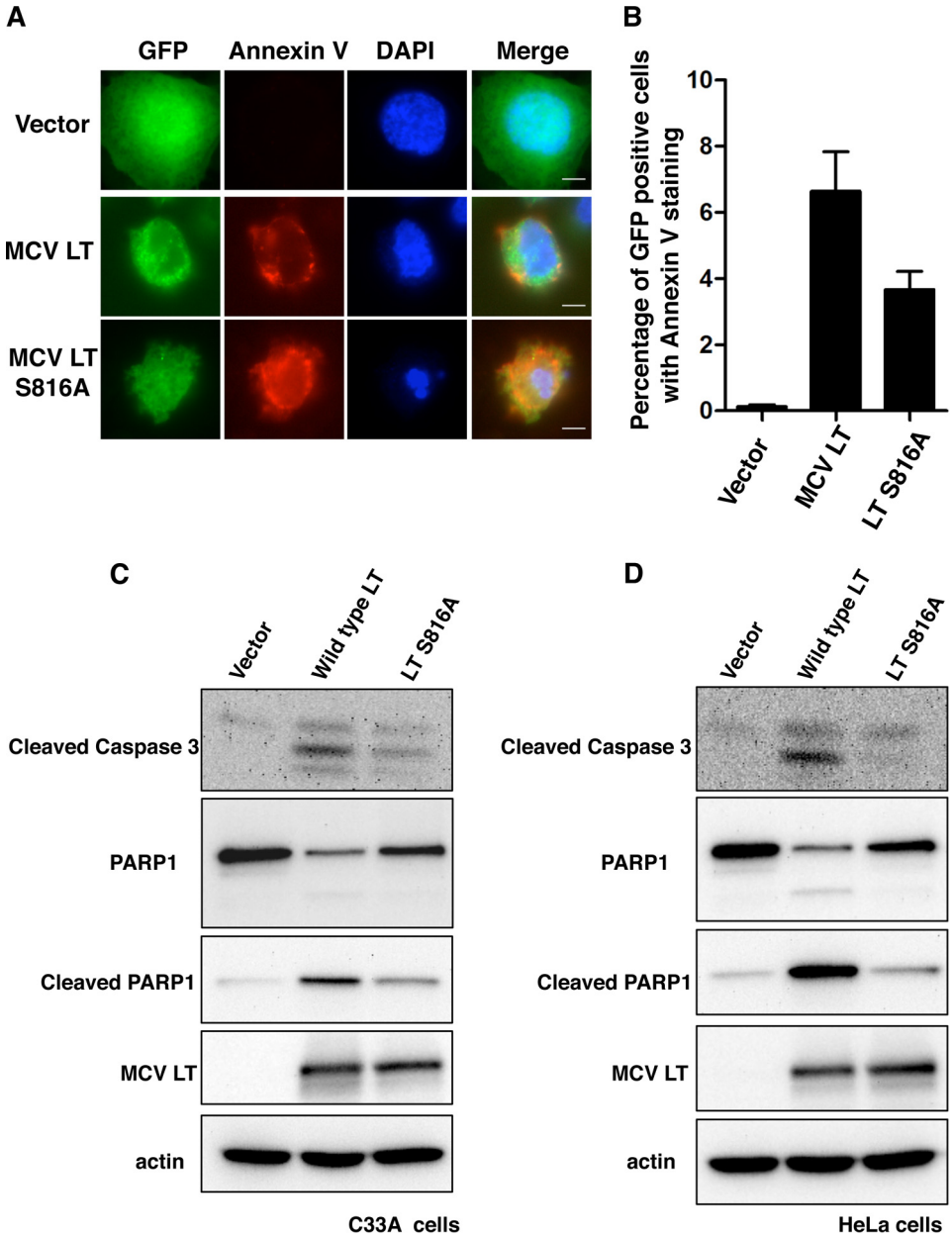

FIGURE 6. **MCV LT induces more apoptosis compared with MCV LT S816A.** *A*, C33A cells were transfected with pEGFPC1 (*Vector*), pEGFPC1-MCV LT, or pEGFPC1-MCV LT S816A. 24 h later, cells were stained with phycoerythrin-conjugated annexin V and DAPI. Images are representative of at least three experiments. *Scale bars* = 10 μm. *B*, the percentage of GFP-positive cells with annexin V staining was quantified from ~100 cells. The mean ± S.D. was calculated from three coverslips. *C* and *D*, C33A and HeLa cells, respectively, were transfected with pcDNA4C (*Vector*), pcDNA4C-MCV LT, or pcDNA4C-MCV LT S816A. Cells were harvested at 30 h post-transfection, and cell lysates were analyzed by Western blotting with the indicated antibodies.

interaction remains elusive. ATM is a serine/threonine protein kinase that is recruited to and activated by dsDNA breaks to phosphorylate several key cellular proteins that initiate activation of the DNA damage checkpoint (52–54). This checkpoint activation results in the phosphorylation and activation of p53, which in turn up-regulates the expression of key cellular factors involved in cell cycle arrest, DNA repair, and apoptosis (52–54). The cell proliferation effects reported here when MCV LT is expressed could therefore be partially due to ATM activity and represent a host response to foreign DNA replication. Indeed, the effects of blocking MCV LT Ser-816 phosphorylation on cell proliferation are modest, and LT S816A was unable to fully rescue the proliferative defect in C33A cells stably expressing LT (Fig. 5), indicating that Ser-816 phosphorylation-independent mechanisms are at play.

Our previous report (16) and present study (Fig. 3*A*) show that transfected LT induces only a very low level of ATM activation. In contrast to transfected LT alone, infection with MCV virions or transfection of viral genomes robustly activates ATM (16); additionally, LT protein levels increase over time in these settings (data not shown). Therefore, during true infection, the ATM-mediated MCV LT Ser-816 phosphorylation may lead to a more robust cell cycle arrest and apoptotic phenotype, which may be advantageous in dispersing newly formed virions late in infection. Alternatively, this ATM-mediated MCV LT Ser-816 phosphorylation and associated apoptotic activities may repre-

sent a host antiviral defense mechanism for eliminating MCV-infected cells.

It is also important to note that we examined only LT when it was expressed alone. Whether LT phosphorylation is altered or temporally regulated when coexpressed with other viral proteins, such as the small tumor antigen, 57kT, or ALTO (alternate frame of the large T open reading frame), remains to be explored. Our previous study established the DDR machinery as critical for LT-mediated viral replication (27). This study further established an intimate interaction between MCV infection and the host DDR, revealing how activation of a host DDR by MCV is then utilized by the virus to carefully orchestrate key events in host cells. Future studies will investigate the downstream events of MCV LT Ser-816 phosphorylation by identifying the cellular proteins that may recognize this phosphorylation event. The identification of the Ser-816 phosphorylation site and the commercial availability of an antibody recognizing this modification provide valuable tools for advancing our understanding of MCV-host interactions.

Acknowledgments—We thank the members of our laboratory for helpful discussions and critical review of this manuscript.

REFERENCES

1. Feng, H., Shuda, M., Chang, Y., and Moore, P. S. (2008) Clonal integration of a polyomavirus in human Merkel cell carcinoma. *Science* **319,** 1096–1100
2. Gjoerup, O., and Chang, Y. (2010) Update on human polyomaviruses and cancer. *Adv. Cancer Res.* **106,** 1–51
3. Shuda, M., Feng, H., Kwun, H. J., Rosen, S. T., Gjoerup, O., Moore, P. S., and Chang, Y. (2008) T antigen mutations are a human tumor-specific signature for Merkel cell polyomavirus. *Proc. Natl. Acad. Sci. U.S.A.* **105,** 16272–16277
4. Kassem, A., Schöpflin, A., Diaz, C., Weyers, W., Stickeler, E., Werner, M., and Zur Hausen, A. (2008) Frequent detection of Merkel cell polyomavirus in human Merkel cell carcinomas and identification of a unique deletion in the *VP1* gene. *Cancer Res.* **68,** 5009–5013
5. Lemos, B., and Nghiem, P. (2007) Merkel cell carcinoma: more deaths but still no pathway to blame. *J. Invest. Dermatol.* **127,** 2100–2103
6. Agelli, M., and Clegg, L. X. (2003) Epidemiology of primary Merkel cell carcinoma in the United States. *J. Am. Acad. Dermatol.* **49,** 832–841
7. Bichakjian, C. K., Lowe, L., Lao, C. D., Sandler, H. M., Bradford, C. R., Johnson, T. M., and Wong, S. L. (2007) Merkel cell carcinoma: critical review with guidelines for multidisciplinary management. *Cancer* **110,** 1–12
8. Schrama, D., Ugurel, S., and Becker, J. C. (2012) Merkel cell carcinoma: recent insights and new treatment options. *Curr. Opin. Oncol.* **24,** 141–149
9. Tolstov, Y. L., Pastrana, D. V., Feng, H., Becker, J. C., Jenkins, F. J., Moschos, S., Chang, Y., Buck, C. B., and Moore, P. S. (2009) Human Merkel cell polyomavirus infection II. MCV is a common human infection that can be detected by conformational capsid epitope immunoassays. *Int. J. Cancer* **125,** 1250–1256
10. Schowalter, R. M., Pastrana, D. V., Pumphrey, K. A., Moyer, A. L., and Buck, C. B. (2010) Merkel cell polyomavirus and two previously unknown polyomaviruses are chronically shed from human skin. *Cell Host Microbe* **7,** 509–515
11. Foulongne, V., Sauvage, V., Hebert, C., Dereure, O., Cheval, J., Gouilh, M. A., Pariente, K., Segondy, M., Burguière, A., Manuguerra, J. C., Caro, V., and Eloit, M. (2012) Human skin microbiota: high diversity of DNA viruses identified on the human skin by high throughput sequencing. *PLoS ONE* **7,** e38499
12. Feng, H., Kwun, H. J., Liu, X., Gjoerup, O., Stolz, D. B., Chang, Y., and Moore, P. S. (2011) Cellular and viral factors regulating Merkel cell polyomavirus replication. *PLoS ONE* **6,** e22468
13. Carter, J. J., Daugherty, M. D., Qi, X., Bheda-Malge, A., Wipf, G. C., Robinson, K., Roman, A., Malik, H. S., and Galloway, D. A. (2013) Identification of an overprinting gene in Merkel cell polyomavirus provides evolutionary insight into the birth of viral genes. *Proc. Natl. Acad. Sci. U.S.A.* **110,** 12744–12749
14. Wang, X., Li, J., Schowalter, R. M., Jiao, J., Buck, C. B., and You, J. (2012) Bromodomain protein Brd4 plays a key role in Merkel cell polyomavirus DNA replication. *PLoS Pathog.* **8,** e1003021
15. Demetriou, S. K., Ona-Vu, K., Sullivan, E. M., Dong, T. K., Hsu, S. W., and Oh, D. H. (2012) Defective DNA repair and cell cycle arrest in cells expressing Merkel cell polyomavirus T antigen. *Int. J. Cancer* **131,** 1818–1827
16. Li, J., Wang, X., Diaz, J., Tsang, S. H., Buck, C. B., and You, J. (2013) Merkel cell polyomavirus large T antigen disrupts host genomic integrity and inhibits cellular proliferation. *J. Virol.* **87,** 9173–9188
17. Hahn, W. C., Counter, C. M., Lundberg, A. S., Beijersbergen, R. L., Brooks, M. W., and Weinberg, R. A. (1999) Creation of human tumour cells with defined genetic elements. *Nature* **400,** 464–468
18. Cheng, J., DeCaprio, J. A., Fluck, M. M., and Schaffhausen, B. S. (2009) Cellular transformation by simian virus 40 and murine polyoma virus T antigens. *Semin. Cancer Biol.* **19,** 218–228
19. Harris, K. F., Christensen, J. B., and Imperiale, M. J. (1996) BK virus large T antigen: interactions with the retinoblastoma family of tumor suppressor proteins and effects on cellular growth control. *J. Virol.* **70,** 2378–2386
20. Shivakumar, C. V., and Das, G. C. (1996) Interaction of human polyomavirus BK with the tumor-suppressor protein p53. *Oncogene* **13,** 323–332
21. Bollag, B., Prins, C., Snyder, E. L., and Frisque, R. J. (2000) Purified JC virus T and T′ proteins differentially interact with the retinoblastoma family of tumor suppressor proteins. *Virology* **274,** 165–178
22. Poulin, D. L., Kung, A. L., and DeCaprio, J. A. (2004) p53 targets simian virus 40 large T antigen for acetylation by CBP. *J. Virol.* **78,** 8245–8253
23. Houben, R., Adam, C., Baeurle, A., Hesbacher, S., Grimm, J., Angermeyer, S., Henzel, K., Hauser, S., Elling, R., Bröcker, E. B., Gaubatz, S., Becker, J. C., and Schrama, D. (2012) An intact retinoblastoma protein-binding site in Merkel cell polyomavirus large T antigen is required for promoting growth of Merkel cell carcinoma cells. *Int. J. Cancer* **130,** 847–856
24. Cheng, J., Rozenblatt-Rosen, O., Paulson, K. G., Nghiem, P., and DeCaprio, J. A. (2013) Merkel cell polyomavirus large T antigen has growth-promoting and inhibitory activities. *J. Virol.* **87,** 6118–6126
25. Borchert, S., Czech-Sioli, M., Neumann, F., Schmidt, C., Wimmer, P., Dobner, T., Grundhoff, A., and Fischer, N. (2014) High-affinity Rb binding, p53 inhibition, subcellular localization, and transformation by wild-type or tumor-derived shortened Merkel cell polyomavirus large T antigens. *J. Virol.* **88,** 3144–3160
26. Kwun, H. J., Guastafierro, A., Shuda, M., Meinke, G., Bohm, A., Moore, P. S., and Chang, Y. (2009) The minimum replication origin of Merkel cell polyomavirus has a unique large T-antigen loading architecture and requires small T-antigen expression for optimal replication. *J. Virol.* **83,** 12118–12128
27. Tsang, S. H., Wang, X., Li, J., Buck, C. B., and You, J. (2014) Host DNA damage response factors localize to Merkel cell polyomavirus DNA replication sites to support efficient viral DNA replication. *J. Virol.* **88,** 3285–3297
28. McVey, D., Brizuela, L., Mohr, I., Marshak, D. R., Gluzman, Y., and Beach, D. (1989) Phosphorylation of large tumour antigen by Cdc2 stimulates SV40 DNA replication. *Nature* **341,** 503–507
29. Grässer, F. A., Scheidtmann, K. H., Tuazon, P. T., Traugh, J. A., and Walter, G. (1988) *In vitro* phosphorylation of SV40 large T antigen. *Virology* **165,** 13–22
30. Prives, C. (1990) The replication functions of SV40 T antigen are regulated by phosphorylation. *Cell* **61,** 735–738
31. McVey, D., Woelker, B., and Tegtmeyer, P. (1996) Mechanisms of simian virus 40 T-antigen activation by phosphorylation of threonine 124. *J. Virol.* **70,** 3887–3893
32. Shi, Y., Dodson, G. E., Shaikh, S., Rundell, K., and Tibbetts, R. S. (2005) Ataxia-telangiectasia-mutated (ATM) is a T-antigen kinase that controls

SV40 viral replication in vivo. *J. Biol. Chem.* **280,** 40195–40200
33. Shimazu, T., Komatsu, Y., Nakayama, K. I., Fukazawa, H., Horinouchi, S., and Yoshida, M. (2006) Regulation of SV40 large T-antigen stability by reversible acetylation. *Oncogene* **25,** 7391–7400
34. Diaz, J., Wang, X., Tsang, S. H., Jiao, J., and You, J. (2014) Phosphorylation of large T antigen regulates Merkel cell polyomavirus replication. *Cancers* **6,** 1464–1486
35. Ciccia, A., and Elledge, S. J. (2010) The DNA damage response: making it safe to play with knives. *Mol. Cell* **40,** 179–204
36. Schreiber, E., Matthias, P., Müller, M. M., and Schaffner, W. (1989) Rapid detection of octamer binding proteins with 'mini-extracts', prepared from a small number of cells. *Nucleic Acids Res.* **17,** 6419
37. Yang, J., Yu, Y., Hamrick, H. E., and Duerksen-Hughes, P. J. (2003) ATM, ATR and DNA-PK: initiators of the cellular genotoxic stress responses. *Carcinogenesis* **24,** 1571–1580
38. Brown, E. J., and Baltimore, D. (2003) Essential and dispensable roles of ATR in cell cycle arrest and genome maintenance. *Genes Dev.* **17,** 615–628
39. Cimprich, K. A., and Cortez, D. (2008) ATR: an essential regulator of genome integrity. *Nat. Rev. Mol. Cell Biol.* **9,** 616–627
40. Cuadrado, M., Martinez-Pastor, B., Murga, M., Toledo, L. I., Gutierrez-Martinez, P., Lopez, E., and Fernandez-Capetillo, O. (2006) ATM regulates ATR chromatin loading in response to DNA double-strand breaks. *J. Exp. Med.* **203,** 297–303
41. Koopman, G., Reutelingsperger, C. P., Kuijten, G. A., Keehnen, R. M., Pals, S. T., and van Oers, M. H. (1994) Annexin V for flow cytometric detection of phosphatidylserine expression on B cells undergoing apoptosis. *Blood* **84,** 1415–1420
42. Salvesen, G. S. (2002) Caspases: opening the boxes and interpreting the arrows. *Cell Death Differ.* **9,** 3–5
43. Ghavami, S., Hashemi, M., Ande, S. R., Yeganeh, B., Xiao, W., Eshraghi, M., Bus, C. J., Kadkhoda, K., Wiechec, E., Halayko, A. J., and Los, M. (2009) Apoptosis and cancer: mutations within caspase genes. *J. Med. Genet.* **46,** 497–510
44. Porter, A. G., and Jänicke, R. U. (1999) Emerging roles of caspase-3 in apoptosis. *Cell Death Differ.* **6,** 99–104
45. Katunuma, N., Matsui, A., Le, Q. T., Utsumi, K., Salvesen, G., and Ohashi, A. (2001) Novel procaspase-3 activating cascade mediated by lysoapoptases and its biological significances in apoptosis. *Adv. Enzyme Regul.* **41,** 237–250
46. Li, P., Nijhawan, D., and Wang, X. (2004) Mitochondrial activation of apoptosis. *Cell* **116,** S57–S59
47. Chaitanya, G. V., Steven, A. J., and Babu, P. P. (2010) PARP-1 cleavage fragments: signatures of cell-death proteases in neurodegeneration. *Cell Commun. Signal.* **8,** 31
48. D'Amours, D., Sallmann, F. R., Dixit, V. M., and Poirier, G. G. (2001) Gain-of-function of poly(ADP-ribose) polymerase-1 upon cleavage by apoptotic proteases: implications for apoptosis. *J. Cell Sci.* **114,** 3771–3778
49. Kaufmann, S. H., Desnoyers, S., Ottaviano, Y., Davidson, N. E., and Poirier, G. G. (1993) Specific proteolytic cleavage of poly(ADP-ribose) polymerase: an early marker of chemotherapy-induced apoptosis. *Cancer Res.* **53,** 3976–3985
50. Tewari, M., Quan, L. T., O'Rourke, K., Desnoyers, S., Zeng, Z., Beidler, D. R., Poirier, G. G., Salvesen, G. S., and Dixit, V. M. (1995) Yama/CPP32β, a mammalian homolog of CED-3, is a CrmA-inhibitable protease that cleaves the death substrate poly(ADP-ribose) polymerase. *Cell* **81,** 801–809
51. Fradet-Turcotte, A., Vincent, C., Joubert, S., Bullock, P. A., and Archambault, J. (2007) Quantitative analysis of the binding of simian virus 40 large T antigen to DNA. *J. Virol.* **81,** 9162–9174
52. Barlow, C., Brown, K. D., Deng, C. X., Tagle, D. A., and Wynshaw-Boris, A. (1997) Atm selectively regulates distinct p53-dependent cell-cycle checkpoint and apoptotic pathways. *Nat. Genet.* **17,** 453–456
53. Abraham, R. T. (2001) Cell cycle checkpoint signaling through the ATM and ATR kinases. *Genes Dev.* **15,** 2177–2196
54. Zhou, B. B., and Elledge, S. J. (2000) The DNA damage response: putting checkpoints in perspective. *Nature* **408,** 433–439